DOT/FAA/TC-12/14

Federal Aviation Administration
William J. Hughes Technical Center
Aviation Research Division
Atlantic City International Airport
New Jersey 08405

Damage Progression in Composite Sandwich Structures due to Fluid Ingression

June 2014

Final Report

This document is available to the U.S. public through the National Technical Information Services (NTIS), Springfield, Virginia 22161.

This document is also available from the Federal Aviation Administration William J. Hughes Technical Center at actlibrary.tc.faa.gov.

U.S. Department of Transportation
Federal Aviation Administration

NOTICE

This document is disseminated under the sponsorship of the U.S. Department of Transportation in the interest of information exchange. The U.S. Government assumes no liability for the contents or use thereof. The U.S. Government does not endorse products or manufacturers. Trade or manufacturers' names appear herein solely because they are considered essential to the objective of this report. The findings and conclusions in this report are those of the author(s) and do not necessarily represent the views of the funding agency. This document does not constitute FAA policy. Consult the FAA sponsoring organization listed on the Technical Documentation page as to its use.

This report is available at the Federal Aviation Administration William J. Hughes Technical Center's Full-Text Technical Reports page: actlibrary.tc.faa.gov in Adobe Acrobat portable document format (PDF).

Technical Report Documentation Page

1. Report No.	2. Government Accession No.	3. Recipient's Catalog No.
DOT/FAA/TC-12/14		

4. Title and Subtitle	5. Report Date
DAMAGE PROGRESSION IN COMPOSITE SANDWICH STRUCTURES DUE TO FLUID INGRESSION	June 2014
	6. Performing Organization Code
7. Author(s)	8. Performing Organization Report No.
John S. Tomblin and Allison Bonitati	
9. Performing Organization Name and Address	10. Work Unit No. (TRAIS)
Wichita State University 1845 Fairmount Wichita, KS 67260-0093	11. Contract or Grant No.
12. Sponsoring Agency Name and Address	13. Type of Report and Period Covered
U.S. Department of Transportation Federal Aviation Administration Northwest Mountain Region – Transport Airplane Directorate 1601 Lind Avenue, SW Renton, WA 98057	Final Report
	14. Sponsoring Agency Code
	AIR-110

15. Supplementary Notes

The Federal Aviation Administration William J. Hughes Technical Center Aviation Research Division Technical Monitor was David Westlund.

16. Abstract

Fluid ingression is free water or fluid that propagates easily through damaged facesheets of sandwich panels, also known as skins. Often this occurs near damaged edges or penetrations through panels where seals are degraded or damaged. This research studied the damage propagation in honeycomb sandwich structures due to water that migrated there after initial impact damage. Panels from a Beechcraft Starship aircraft and representative panels from an Adam Aircraft business jet were subjected to nominal thermal cycling of -65° to 180°F, and the initial impact damage growth was measured using ultrasonic inspection. Three different tests were performed in which (1) the panels were initially soaked for 1 hour in 180°F water, (2) the panels were initially soaked for 2 hours in 180°F water, and (3) a constant tension load was applied to the panel. The panels were impacted to create barely visible damage, visible damage, and severe damage. The results of all tests showed that the damage initially grew approximately 20%, up to 1000 cycles, and then was arrested, independent of the severity of the initial damage. Further cycling of up to 5000 cycles did not increase the damage. The initial impact damage was facesheet-to-core interface and core crushing at higher impact levels. After cycling, the damage growth was additional core breakage caused by water freeze/thaw cycles. The cycling represented ground-air-ground cycles experienced by aircraft. Pressure differential was not simulated as it was assumed that the impact damage was substantial enough to penetrate the skins.

17. Key Words	18. Distribution Statement
Fluid ingression, Composite sandwich structures, Impact damage, Thermal cycling, Damage progression	This document is available to the U.S. public through the National Technical Information Service (NTIS), Springfield, Virginia 22161. This document is also available from the Federal Aviation Administration William J. Hughes Technical Center at actlibrary.tc.faa.gov.

19. Security Classif. (of this report)	20. Security Classif. (of this page)	21. No. of Pages	22. Price
Unclassified	Unclassified	38	

Form DOT F 1700.7 (8-72) Reproduction of completed page authorized

ACKNOWLEDGEMENTS

The authors would like to express their appreciation to Hal Loken and Peter Shyprykevich for their insight on the mechanics of fluid ingression and to Larry B. Ilcewitcz for his program support.

TABLE OF CONTENTS

		Page
EXECUTIVE SUMMARY		ix
1.	INTRODUCTION	1
2.	BACKGROUND	2
3.	TEST METHODOLOGY	8
	3.1 Scope and Procedures	8
	3.2 Impact Tests	9
	3.3 Thermal Soak and Cycling	9
4.	TEST RESULTS	13
	4.1 Starship Panel Results, 1-Hour Bath	14
	4.2 Adam Panel Results, 1-Hour Bath	16
	4.3 Starship and Adam Panels Under Thermal Cycling, 2-Hour Bath	19
	4.4 Starship and Adam Panels Under Load and Thermal Cycling	21
5.	CONCLUSIONS	28
6.	FUTURE WORK	28
7.	REFERENCES	29

LIST OF FIGURES

Figure		Page
1	Basic Honeycomb Sandwich Structure	1
2	Developing Microcracks in a Sandwich Panel	3
3	Airbus A300 Aircraft With Composite Rudder	3
4	Airbus A300 Rudder Removed From Aircraft	4
5	Inside A300 Rudder With Fluid Ingression Present	4
6	Thin-Skin Facesheets	5
7	The Starship Fuselage	6
8	Location of Representative Adam Aircraft Panels	7
9	Cut Diagram for Obtaining Test Panels	7
10	Impact Drop Tower Diagram	9
11	A 3″ Diameter Tup Used to Impact Sandwich Panels	9
12	Test Panels in Water Bath	10
13	Environmental Chamber Output	11
14	A Four-Point Bend Fixture for Damaged Sandwich Panels	12
15	Panel B12 Ready for Thermal Cycling	12
16	Test Panel Preparation for Panels Under Load	13
17	Starship Panel Damage at Three Different Impact Levels	14
18	Adam Panel Damage at Three Different Impact Levels	14
19	Damage Area vs. GAG Cycle Count for Starship Panels	15
20	Starship Panel B16 Damaged Area, 0 Thermal Cycles	15
21	Starship Panel B16 Damaged Area, 2000 Thermal Cycles	16
22	Cross-Section of a Typical Damaged Panel Before GAG Cycling	16
23	Damage Area vs. GAG Cycle Count for Adam Panels	17
24	Adam Panel CP3 6B, 0 Thermal Cycles	18
25	Adam Panel CP3 6B, 2000 Thermal Cycles	18
26	Adam Panel CP6 4D, 0 Thermal Cycles	19
27	Adam Panel CP6 4D, 2000 Thermal Cycles	19
28	Damage Area vs. Cycles for Starship Panels, 2-Hour Bath	20
29	Damage Area vs. Cycles for Adam Panels, 2-Hour Soak	20
30	The Four-Point Bend Fixture and Free Body Diagram	21
31	Damage Area vs. Cycles for the Starship Panel C11, Under Load	22
32	Starship Panel C11 After Impact, 0 Thermal Cycles	22
33	Starship Panel C11 After Impact, 500 Thermal Cycles	23
34	Starship Panel C11 After Impact, 1000 Thermal Cycles	23
35	Starship Panel C11 After Impact, 5000 Thermal Cycles	23
36	Damage Area vs. Cycles for Starship Panels Under Load	24
37	Damage Area vs. Cycles for Adam Panels Under Load	25
38	Starship Panel C14; 0, 100, and 500 GAG Cycles	25
39	Starship Panel C18; 0, 100, and 500 GAG Cycles	26
40	Starship Panel B12; 0, 100, and 500 GAG Cycles	26
41	Adam Panel CP3 2D; 0, 100, and 500 GAG Cycles	27
42	Adam Panel CP8 C6; 0, 100, and 500 GAG Cycles	27
43	Adam Panel CP8 B4; 0, 100, and 500 GAG Cycles	28

LIST OF TABLES

Table		Page
1	Starship Panels No Loading Damage Area	14
2	Adam Panels No Loading Damage Area	17
3	Starship Panels Test Results Under Thermal Cycling and 2-Hour Bath	19
4	Adam Panels Test Results Under Thermal Cycling and 2-Hour Bath	20
5	Starship Panel C11 Results Under Load	21
6	Starship and Adam Panels; Four-Point Loading, Thermal Cycle Results	24

LIST OF ACRONYMS

BVID	Barely visible impact damage
GAG	Ground-air-ground
NDI	Nondestructive inspection
NDT	Nondestructive transmission
VID	Visible impact damage

EXECUTIVE SUMMARY

Honeycomb sandwich composite structures are commonly used in the aerospace industry. They offer lightweight, stiff-beam construction that is well-suited for many aircraft parts. The sandwich construction makes these parts lighter than solid laminate construction. However, the sandwich structure can be easily punctured, as the facesheets are thinner, providing paths for fluid ingression.

This research on the effect of fluid ingression in sandwich structures was based on the assumption that the damage to the sandwich structure already exists. This was simulated by impacting all test articles to three damage levels: barely visible, visible, and severe. With the fluid in the damaged area, the effects that thermal and mechanical loads have on a sandwich structure under these conditions were then studied. This is defined as the damage tolerance approach to the fluid ingression problem.

Panels from a Beechcraft Starship aircraft and representative panels from an Adam Aircraft business jet were subjected to nominal thermal cycling of -65° to 180°F, and the initial impact damage growth was measured using ultrasonic inspection. Three different tests were performed in which (1) the panels were initially soaked for 1 hour in 180°F water, (2) the panels were initially soaked for 2 hours in 180°F water, and (3) a constant tension load was applied to the panel. The results of all the tests showed that the damage initially grew approximately 20%, up to 1000 cycles, and then was arrested, independent of the severity of the initial damage. Further cycling of up to 5000 cycles did not increase the damage. The initial impact damage was facesheet-to-core interface and core crushing at higher impact levels. After cycling, the damage growth was core breakage caused by water freeze/thaw cycles. The cycling represented ground-air-ground cycles experienced by aircraft. The pressure differential was not simulated as it was assumed that the impact damage was substantial enough to penetrate the skins.

1. INTRODUCTION.

Honeycomb sandwich composite structures are very useful in the aerospace industry. They offer a lightweight, stiff-beam construction that can be valuable in several applications. The sandwich composite material makes these parts lightweight; however, the sandwich material can be damaged more easily than solid composite laminates. Although there are other materials that can provide stiffness without adding significant weight, this research focused on honeycomb sandwich structures. These types of sandwich laminates are ideal for control surfaces. They also prevent water and fluid ingress [1].

Figure 1 shows a basic schematic of the elements of sandwich construction in which the facesheets support the in-plane loads (tension/compression) and the core support the shear loads. The core, although stiff in nature, is very brittle. The composite facesheet consists of a reinforcement and matrix material. Carbon, glass, and aramid fibers are all reinforcements infused with epoxy resin. This research was on carbon fiber with an epoxy resin matrix facesheet and honeycomb core.

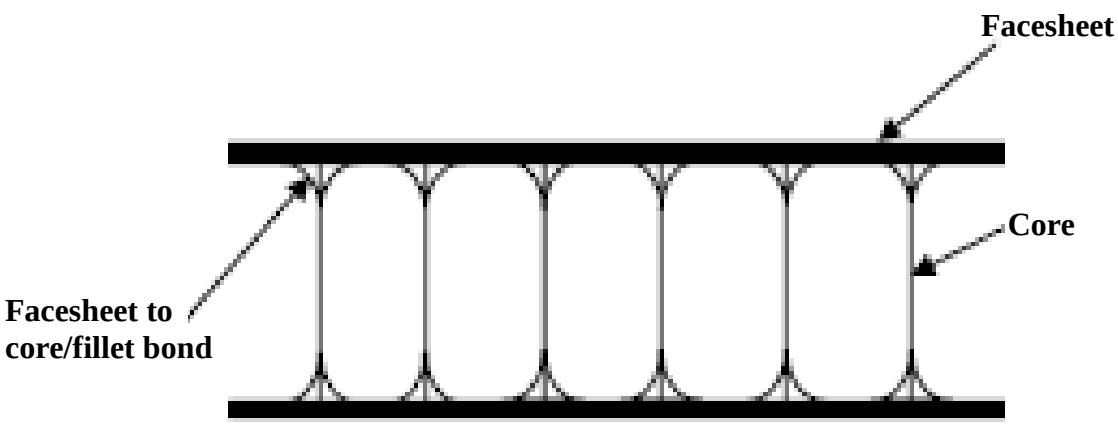

Figure 1. Basic Honeycomb Sandwich Structure

Damage can occur to a facesheet during manufacturing, repair, lightning strikes, bird strikes, and hail. If the sandwich core becomes damaged, the part integrity could then be compromised. This is a concern because the environmental durability of sandwich core is very poor. The facesheet or outer skin of a sandwich structure can be subjected to many fluids, both on the interior and exterior of an aircraft, during service. Because the combination of fluids with thermal and mechanical loads causes degradation to the sandwich structure over time, they are a closed structure by design. Despite the closed design, sandwich structures have been known to absorb moisture, which results in increased weight gain, degradation of the core and facesheet materials, and degradation of the core-to-facesheet interface bond [2-6]. It is important to understand the fluid ingression paths and damage mechanisms that result in decreased structural performance as related to continued airworthiness of the aircraft.

Fluid ingression is free water or fluid that propagates easily through damaged facesheets and skins near the edges, near penetrations through panels where seals are degraded or damaged, through rivet holes or impact damage, or by diffusion through the epoxy matrix on the composite

skin, particularly in the case of thin facesheets. Fluid ingression is not a problem that results from the switch from aluminum alloy to composite airframes. Fluid ingression can easily be understood and avoided given the right design and aircraft maintenance.

2. BACKGROUND.

Some research has been performed on the durability of honeycomb cores, but not on how fluid ingress affects structural integrity over time. The four most common cores are Nomex®, Korex® (Kevlar® core), glass fiber, and aluminum. Cores provide shear strength, flatwise compression, and flexural strength to a structure. These are the three most common design characteristics used when designing a part with core of any kind. The University of Washington performed several studies on the longtime water exposure on the durability of honeycomb cores. Over a 38-week period, the Nomex core absorbed the most water, followed by Korex, glass fiber, and then aluminum cores [2]. Several tests were done on the core samples while they were soaking in water for the 38-week duration. Overall, aluminum core delamination strength decreased the most; no significant change was prevalent in the flexural or compressive strength, except in the machined direction of the cores. During the 38 weeks, the cores retained anywhere from 0.26 to 7.0 wt.% of water [2]. These results are not unexpected because all cores absorb some water after being exposed to fluid over a long period of time.

Thermal and mechanical cycling cause stresses in a composite sandwich structure. Often, these stresses are relieved through the presence of microcracks that develop in the paint and reinforcement matrix. Cracks that run parallel to the fiber are particularly harmful to the facesheets. Research at DuPont® has shown that these types of cracks are more commonly found in carbon fiber and aramid fiber (Kevlar) facesheets. An example of parallel-running cracks is shown in figure 2. The thermal and moisture cycling create minor micromechanical stresses because of the constant expanding and contracting of the sandwich part. The amount of expansion that occurs is dependent on a unique correlation between the reinforcement material and facesheet ply orientations, temperatures the part is exposed to, and thermal expansion coefficient of the reinforcement matrix [7].

This potential problem is focused primarily on aircraft that operate routinely at high and low temperatures (-65° to +100°F) while traveling from ground level to a maximum flight ceiling of 40,000 feet [7]. These temperatures and elevations, when cycled continuously, are particularly harsh on sandwich composite parts. In particular, the paint that covers the sandwich part and protects it from the outside environment is primarily susceptible to cracks—including microcracks. The coefficient of thermal expansion for paint is important to consider. If the paint does not have some elasticity to flex slightly with mechanical and thermal loads, the paint will crack very easily, and it will be very easy for fluid to enter the facesheet and, ultimately, the sandwich structure.

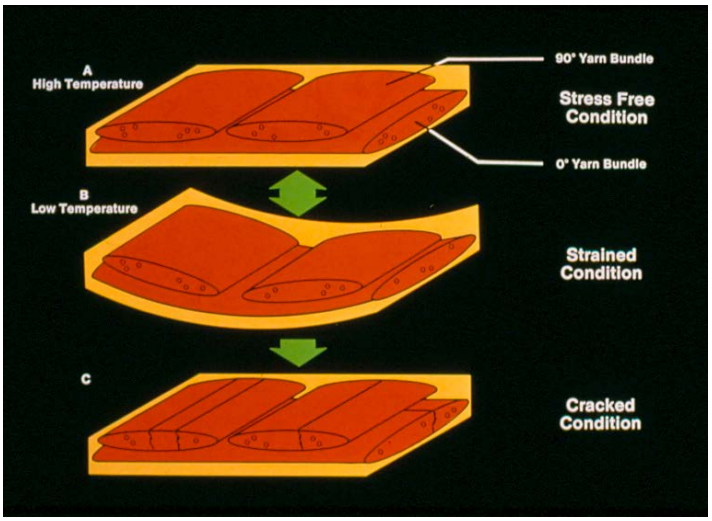

Figure 2. Developing Microcracks in a Sandwich Panel [8]

A number of reports document service problems due to water ingression and describe ways to avoid these types of problems in future designs [6]. For example, in the 1970s, a wide-body transport aircraft experienced fluid ingression on the trailing edge. The cause of the fluid ingression was linked to material properties and performance. The resin content of the prepreg was reduced for weight savings; therefore, the facesheet laminate had channels that directed both Skydrol® and water into the honeycomb sandwich structure. The materials used on this trailing edge were a woven fabric prepreg for the facesheet, a solid laminate for the spar, and an aramid honeycomb for the core. Increasing the prepreg resin content resolved the fluid ingression problem on the trailing edge and highlighted the importance of material performance with respect to fluid ingression.

The Airbus A300 transport aircraft (figure 3) has parts that have had fluid ingression problems. The rudder is manufactured using honeycomb sandwich construction techniques that have proven to be vulnerable to fluid ingression problems in the past. To represent the size and scale of this rudder (a large, one-piece composite part), figure 4 shows an A300 rudder that has been removed from the aircraft.

Figure 3. Airbus A300 Aircraft With Composite Rudder

Figure 4. Airbus A300 Rudder Removed From Aircraft

This structure is composed of typical thin-skin facesheet construction and design details that may increase fluid ingression rates and subsequently degrade the structural performance. Figure 5 shows an inside view of the rudder indicating the fluid ingression that occurred during service.

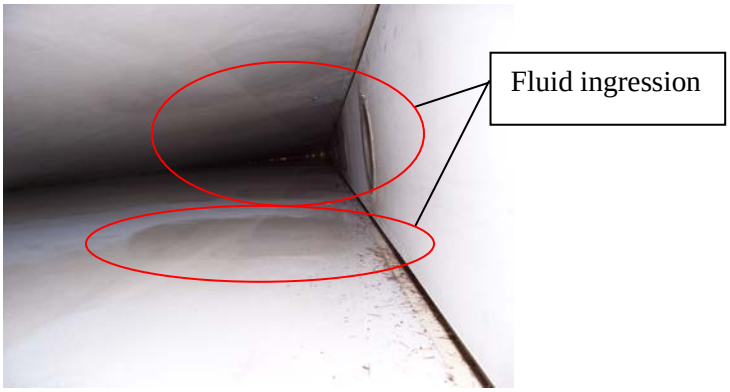

Figure 5. Inside A300 Rudder With Fluid Ingression Present

In addition to the type of fluid ingression caused by design geometry, thin-skin facesheets have also been shown to increase the amount of moisture ingression. There is a significant need to characterize this effect, because existing structural design, maintenance, and repair may act to increase the probability for moisture ingression to occur. The fluid ingression shown in figure 5 is an example of the problems that can occur in honeycomb sandwich construction parts.

Moisture ingression is one scenario of the fluid ingression phenomenon. The rate of moisture ingression is a function of type of damage in the structure. The research performed here concerns the ingress of moisture in a composite sandwich structure that has been damaged by impact.

There are five significant research variables to address while identifying and troubleshooting the damage mechanisms related to fluid ingression:

- Design—construction details, facesheet thickness, fasteners, seals, etc.
- Damage mechanisms—impact, hail, repair, lightning, bird strikes, etc.
- Fluid and material types
- Ingression rates—based on environmental exposure
- Experimental characterization—detailed test plan

Damage size is also affected by facesheet thickness (i.e., the thinner the facesheet, the less impact damage that facesheet will be able to withstand; the thicker the facesheet, the more impact damage that particular facesheet can withstand).

Compared to thick facesheets, thin-skin facesheets (figure 6) present a problem regarding the amount of impact energy they can withstand without being damaged. Upward-facing laminates require special consideration and need to be further investigated because fluid flows more easily into a part with an upward-facing laminate than with a laminate that is shielded by other structures. These upward-facing laminates are the surfaces at the top of the fuselage or wing skins. These areas are more likely to be impacted by hail or lightning, as opposed to the underside of the fuselage or wing skins. These parts are impacted by the water from a storm, but the damage is likely to be less severe with the upward-facing laminates.

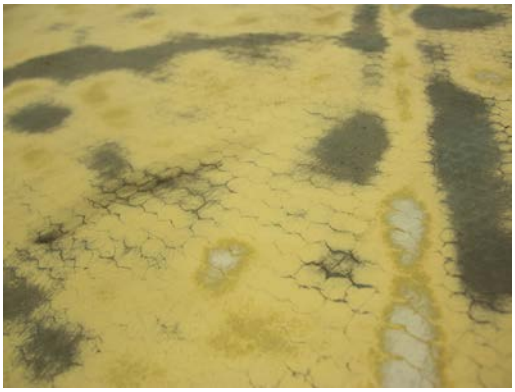

Figure 6. Thin-Skin Facesheets

This report addresses the freeze/thaw cycle effects on fluid ingression and how fast thermal loads propagate fluid ingression. Conditioning of ground-air-ground (GAG) cycles is the most important factor because the volume of water maximizes when it freezes. When water freezes, it adds 9% by volume to each water molecule; this volume increase can damage nodes and cell walls are more easily damaged. The transport aircraft GAG cycle that this and several other researchers use is very conservative, particularly after the hot/wet condition reaches above 160°F and the cold/dry condition gets below -55°F. At 180°F, the materials are well above the wet glass transition of most resin systems used today, and at -65°F, the micromechanical transverse tensile stress rises enough to cause the critical tensile strain to be exceeded in more places, creating extensive facesheet microcracks [8].

The technical approach for this research investigated and isolated variables related to fluid ingression in typical honeycomb composite sandwich constructions. The objective of this research was to answer the following questions:

- What are the mechanisms that cause fluid ingression?
- How does discrete source damage propagate?
- How fast do freeze/thaw cycles propagate fluid ingression?
- What is the path for the fluid ingression?

This research focused on traditional impact damage of varying levels of severity. The intention was to determine the level of impact damage relative to the rate of fluid ingression within the structure. Several levels of impact damage were used from barely visible impact damage (BVID) to visible impact damage (VID). Water was the primary fluid used for this investigation.

This investigation focused on existing aircraft structures that were removed from retired aircraft. The structures selected were manufactured with graphite carbon fiber facesheets bonded to a Nomex honeycomb core. This combination is typically used for current structural components in the aircraft manufacturing industry. The decommissioned Beechcraft Starship fuselage and representative Adam Aircraft fuselage skins were selected as test panels. Figure 7 shows a schematic of the decommissioned Starship fuselage.

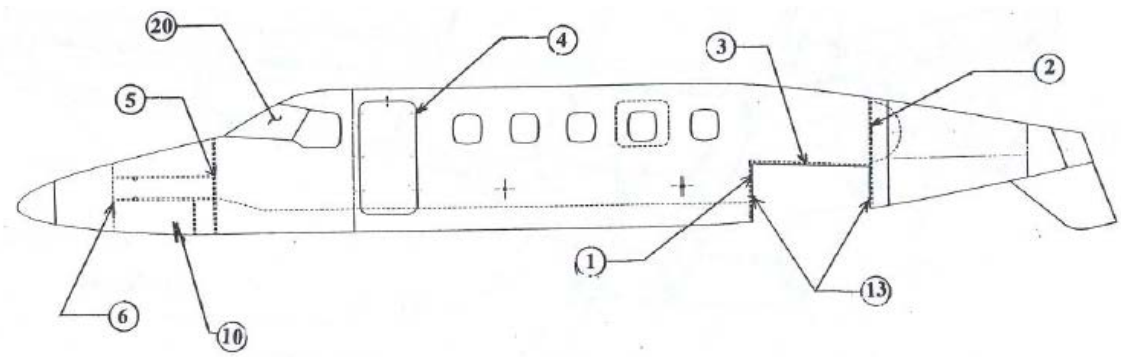

Figure 7. The Starship Fuselage

The Starship is comprised of an AS4 carbon fiber with an E7K8 Cytec resin system and honeycomb core. Subpanels were cut from the fuselage, nose, bulkheads, cargo bay, and bonded-seam areas. The lay-up for the panels was 3 or 4 plies, depending on the location. The types of core were 3.0 lb Nomex or 515 lb flex or fiberglass and the thickness was either ¾ in. or 1 in. Panel sizes for the fuselage averaged 12″ by 16″ for both the Starship and representative Adam Aircraft panels (referred to as Adam panels) (figure 8).

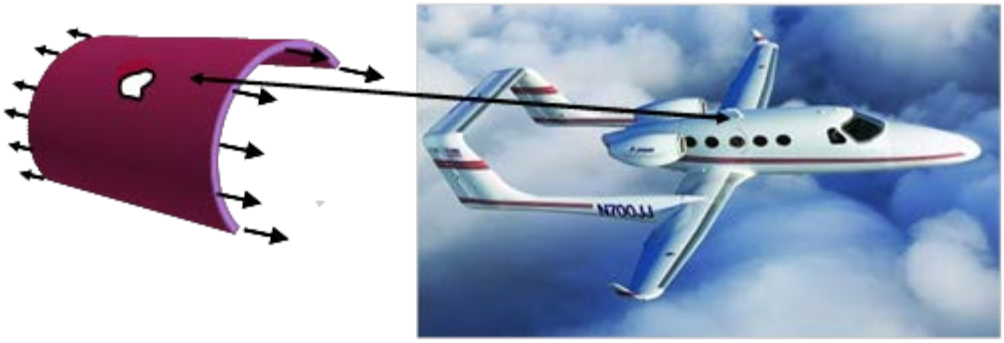

Figure 8. Location of Representative Adam Aircraft Panels

In this report, the decommissioned Beechcraft Starship test panels are referred to as Starship panels. The material systems chosen for the test panels, which are referred to as the representative Adam Aircraft panels, are Toray Composites T700SC-12K-50C/#2510 Plain Weave Carbon fabric for the facesheets and Nomex HRH-10/OX-3/16-3.0 honeycomb of 0.75″ thickness for the core. The lay-up schedule for the test section of the sandwich panel is [45/0/45/Core/45/0/45]. The material systems and stacking sequences are similar to the Adam Aircraft A700 aircraft fuselage structure. The Adam panels were cut as shown in figure 9.

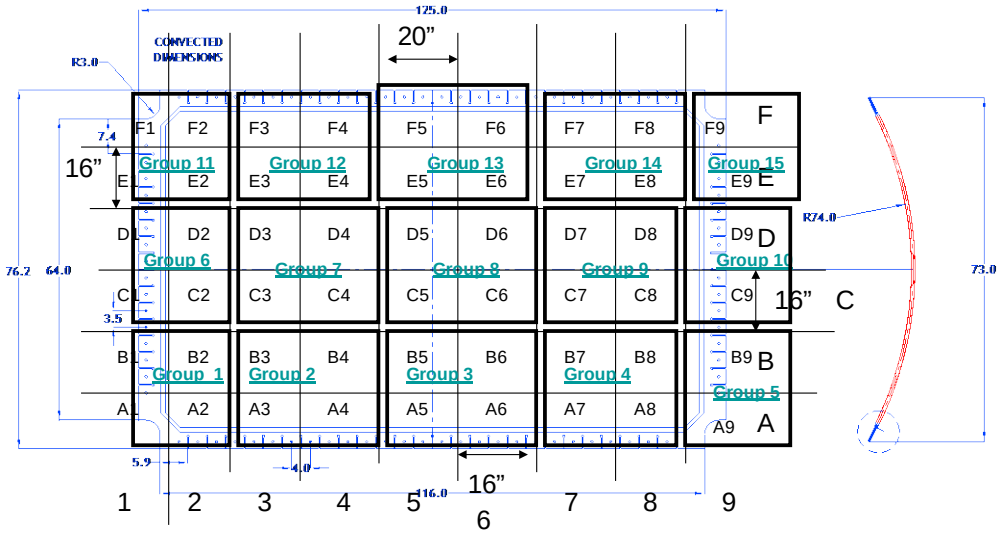

Figure 9. Cut Diagram for Obtaining Test Panels

An impact drop tower was used to damage the panels, using a specific size diameter tup on all panels that provided a uniform damage size with three different damage definitions. BVID, VID, and severe damage are the three target damage levels that were achieved by impacting the test panels. These three impact levels (or damage definitions) were chosen to correlate to actual damage mechanisms that could possibly occur in aircraft operations. Hail, baggage cart, bird strike, and lightning strike damage are a few of the damage mechanisms that can occur to aircraft in everyday operations.

3. TEST METHODOLOGY.

3.1 SCOPE AND PROCEDURES.

Three different sets of specimens were tested for the Starship and Adams panels: one set with 1 hour of thermal bath followed with thermal cycling, one set with 2 hours of thermal bath followed by thermal cycling, and one set under tension loading.

Three levels of impact damage were attained for each panel set: BVID, VID, and severe case. Weights were recorded before the water bath, after the water bath, and before and after each thermal cycling milestone for each panel so that the initial moisture level after the soak was maintained during the cycling tests.

Each panel was inspected by ultrasonic transmission before and after impact so the damage area could be identified. It is important to quantify the amount of initial damage before thermal cycling so, if the damage area grows as a result of thermal cycling, the growth amount can be documented. Ultrasonic inspection was performed after each cycling milestone was completed.

During the tests, the following key variables were measured and recorded:

- Nondestructive transmission (NDT) inspection—Ultrasound images were taken on all panels prior to any other testing. Ultrasonic inspection was repeated after impact damage and after each thermal cycling milestone. The equipment manufacturer was NDT Automation, and the mode used for this test was through transmission ultrasonic at a frequency of 1 MHz.

- Weight measurement—Each panel's weight was recorded in grams before anything else was completed. The weight was recorded again after each thermal cycling milestone was completed.

- Impact energy—As discussed previously, three levels of impact damage were attempted: BVID, moderate damage (damage is visible), and severe (damage was present on top facesheet and core, but bottom facesheet was not damaged). As a result, there were three to four different impact energies per panel type, depending on the panel and facesheet thickness.

- Thermal cycle count—Thermal cycling milestones were established after trial runs were completed on sample test panels. The thermal cycle count established for most of the test matrices were 100, 500, 1000, 2000, and 5000. Not all test matrices reached the anticipated cycle count due to funding and time constraints. All thermal cycling performed was completed within the selected temperature range (-65° to 180°F).

- Digital images—Digital images were taken of all significant changes. Digital images are a reminder and visual indicator of what was done.

- Area—The area measured is the actual damaged area before any thermal cycling and after each thermal cycling milestone is completed.

3.2 IMPACT TESTS.

Panels were impacted using an impact drop tower (figure 10) with a 3″ diameter tup (figure 11). The 3″ diameter tup was chosen over the 1″ diameter tup as it was shown that it creates greater uninspectable damage for honeycomb structures. Several trials were completed to determine which impact energy correlated with the three target damage levels: BVID, VID, and severe. A C-scan of the panel was conducted to provide a baseline of the initial damage.

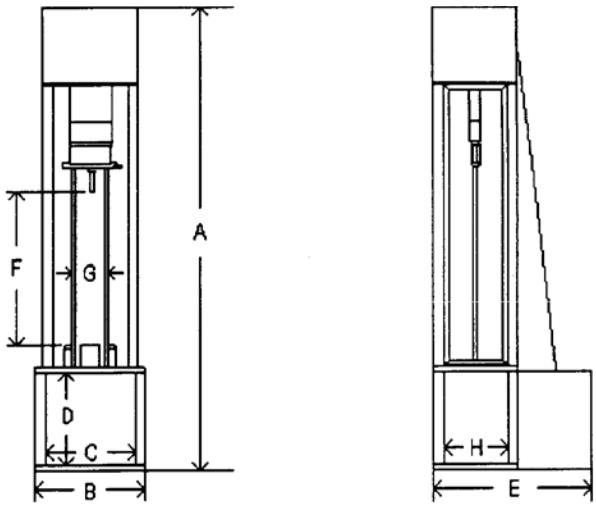

Figure 10. Impact Drop Tower Diagram

Figure 11. A 3″ Diameter Tup Used to Impact Sandwich Panels

As shown in figure 10, the overall height of the impact drop tower (A) is 107 inches, the total width (B) is 23 inches, and the maximum vertical drop height (G) is 46 inches; however, this height varies slightly based on tup diameter and specimen thickness. The impact drop tower manufacturer is Instron® Dynatup®.

3.3 THERMAL SOAK AND CYCLING.

After the test panels were impacted, they were subjected to thermal soak and cycling. The thermal cycling mirrored a commercial transport aircraft GAG cycle. Previous research also

attempted thermal cycling using similar GAG cycles, since it is the best way to subject test panels to actual thermal loads that are experienced in service. However, pressure fluctuations of GAG cycles were not simulated. A pressure differential is created when these parts are installed and working in their operating environment on the aircraft. When the panels are damaged, the pressure differential is lost because there is now a large hole in the once-closed part.

The typical cycle chosen was between -65° and 180°F. The panels were subjected to a 1-hour water bath at 180°F before the thermal cycling began and after each thermal cycling milestone was completed. This was to ensure there was fluid within the damage area of the panel before thermal cycling.

For thermal cycling, each panel was first visually inspected for any obvious damage, and the damage was documented. Since, by design, the parts are closed when manufactured and the test panels were cut from aircraft parts, the edges became exposed. Before thermal soak and cycling, the edges were sealed with high-temperature epoxy caulking and then covered completely with aluminum tape. The damaged panel received a 1- to 2-hour water bath depending on the matrix prior to thermal cycling. This water bath was completed in a tub in a 180°F environmental chamber (figure 12).

Figure 12. Test Panels in Water Bath

On average, the time in the environmental chamber was 91 minutes to complete the cycle from room temperature, to -65°F, up to 180°F, and back to room temperature. This allowed for up to 16 cycles per day. However, with visual inspections, nondestructive inspections (NDI) and weight measurements required, 16 cycles were not completed every day. Each cycle began at room temperature and ramped down to -65°F, causing the fluid present within the damage area to freeze and expand, potentially causing more damage to the core. Next, the chamber was ramped up to 180° from -65°F, where frozen fluid melted and potentially evaporated. Finally, the chamber ramped back down to room temperature from 180°F, and, once at room temperature, one cycle was complete. At this point, visual inspections were routinely performed to verify that there was still some fluid in the damaged core area. Without fluid present, fluid ingression would not be possible with additional thermal cycles. Figure 13 shows an example of the output obtained from the environmental chamber and shows the temperature versus cycle count graphs history. After ten cycles, the weight of the panel was taken. If 25 percent of the weight gained

was lost, the panel was returned to the water bath for 2 hours, prior to another cycle in the environmental chamber.

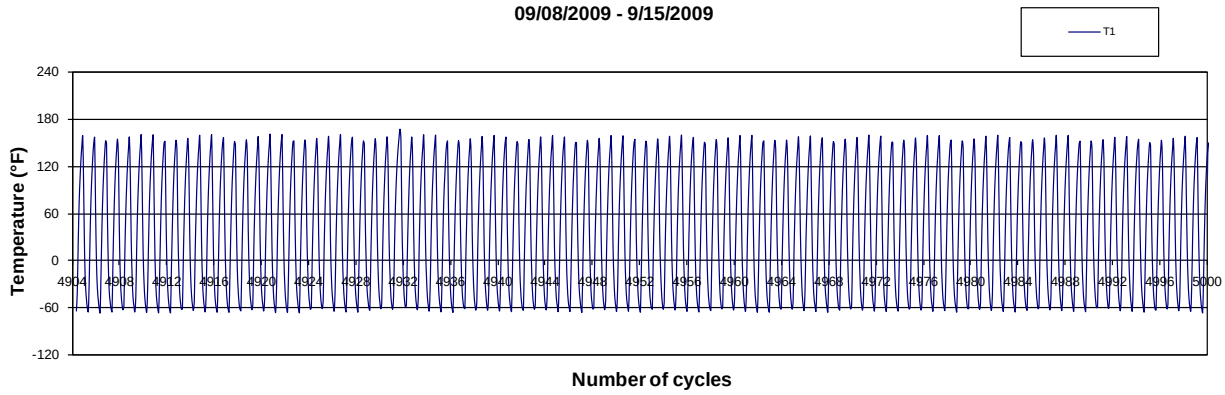

Figure 13. Environmental Chamber Output

Given the number of panels and the milestones selected, the environmental cycling added significant time to this research project. In late 2009 and the beginning of 2010, other options for thermal cycling were explored. A thermal shock chamber was made available in 2010 that would complete a cycle significantly faster than the traditional environmental chamber. In the environmental chamber one can get 16 cycles in one day (approximately 12 hour day) while in the thermal shock chamber one can get 16 cycles in 3.5 hours. At this rate, about 75 cycles per month were accomplished. The 75 cycles per month were an average when using the thermal shock chamber, which was averaging 3.5 hours of cycling in 3.5 hours and produced 16 cycles. Neither the environmental chamber nor thermal shock chamber ran continuously, as chambers did break, which is a significant reason why the number of cycles and rates did not always add up.

There were also modifications made to the temperature control of the thermal shock chamber; this time, the chamber was controlled by a thermocouple inserted inside the damage area. Previously, the thermocouple was placed just outside of the part and the environmental chamber was controlled by air temperature. This modification was done because all that is needed to create fluid ingression is for the fluid in the damage area to freeze and thaw repeatedly; this action creates the necessary damage in the cell walls to create fluid paths. The set points for the thermocouple inside the damage area were -20° and 100°F. The thermocouple inside the damaged area does not have to reach -65° and 180°F; the goal is to make ice and thaw ice in one cycle and this could be achieved with the new set points. The outside air temperatures surrounding the part and the part surface will experience greater temperatures (not recorded) than the thermocouple set points as the thermal shock chamber adjusts to meet the set points, but the material systems of the panels can withstand these temperatures.

For panels under load, a four-point bend fixture was used (figure 14). This fixture was designed to apply a small amount of constant mechanical load, in tension, to the sandwich panels while undergoing thermal cycling. All the panels placed in this fixture were preloaded to 800 microstrains. This was the highest strain that the panel was capable of maintaining without inducing damage to the panel. To help keep the water around the damage area, a rubber dam was used (figure 15).

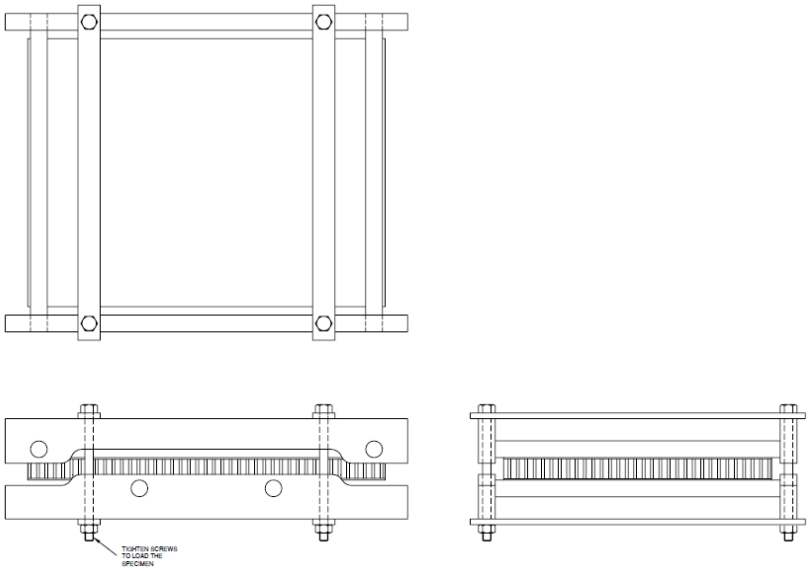

Figure 14. A Four-Point Bend Fixture for Damaged Sandwich Panels

Figure 15. Panel B12 Ready for Thermal Cycling

A strain gage was mounted, using M-Bond 600, on the panels that were subjected to mechanical and thermal loads. This differed from the panels that were only subjected to thermal cycling. The gaged panel was then placed into the water bath to allow the damaged area to be submerged for 1 hour at 180°F. Figure 16 shows a schematic of the panel preparation.

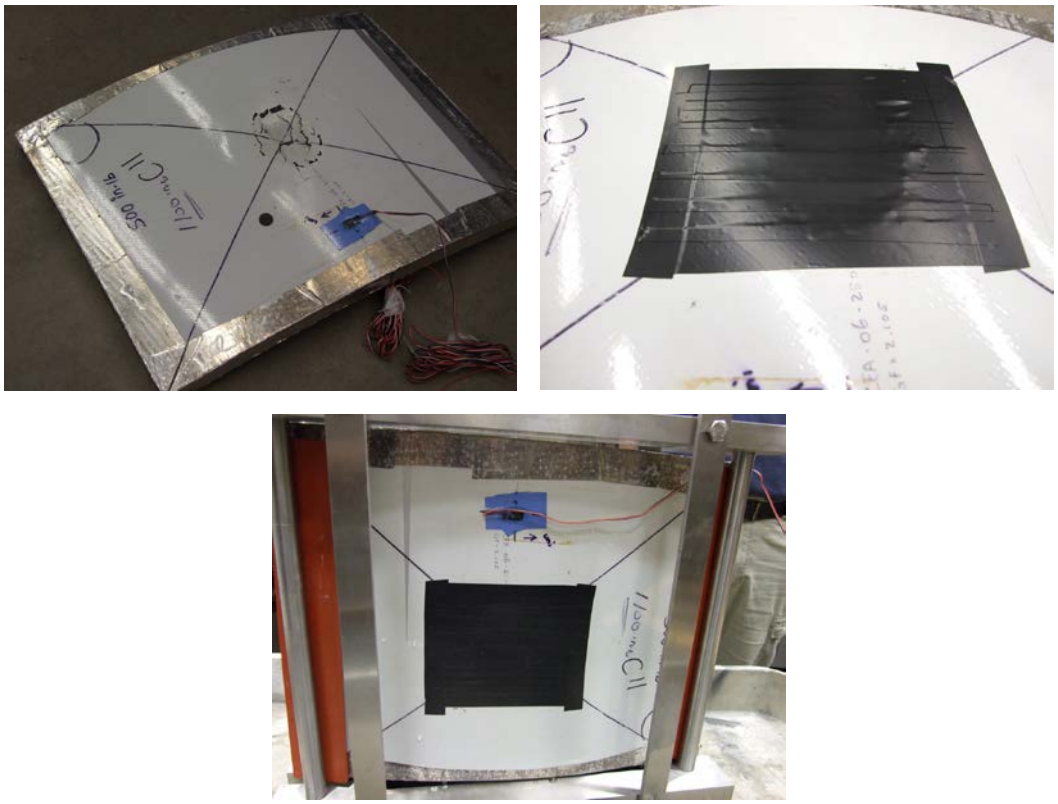

Figure 16. Test Panel Preparation for Panels Under Load

The damaged area was filled with fluid by submerging the panel in the water bath. It was sealed with tape prior to being placed in the four-point bend test fixture, as shown in figure 16. After the water bath, it took about 30 minutes to place the test panel in the fixture, torque the bolts, and prestrain the panel. Then the thermal cycling began. Panel weights were checked after each milestone was completed, and, if needed, the panel was placed back in the water bath for more fluid intake before additional thermal cycling.

4. TEST RESULTS.

For this research, it was assumed that the damage occurred and the fluid was in the sandwich structure. The damage was inflicted by impacting the panels using the impact drop tower described in section 3.2. The three impact levels chosen were based on several trials of sample panels. Figure 17 shows how the three different impact energy levels (BVID, VID, and severe damage) appeared on the Starship panels after impact, and figure 18 shows the effects of three different impact energy levels for the representative Adam panels.

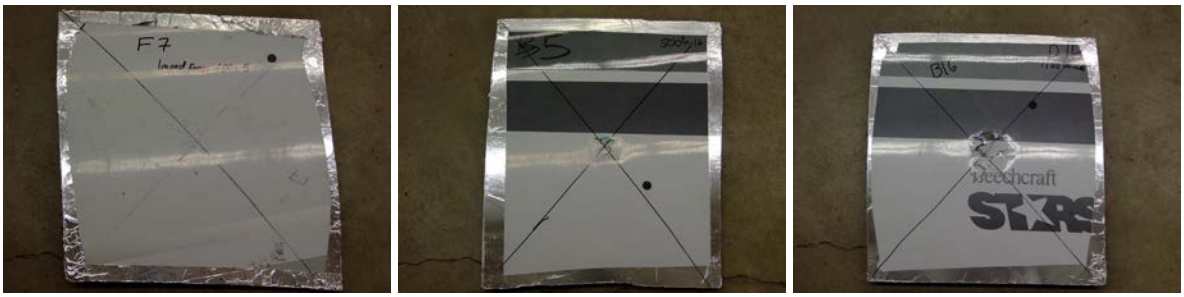

Figure 17. Starship Panel Damage at Three Different Impact Levels

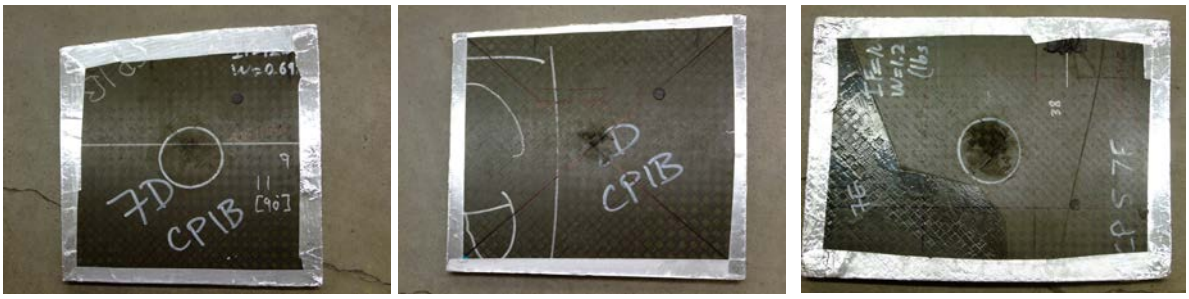

Figure 18. Adam Panel Damage at Three Different Impact Levels

4.1 STARSHIP PANEL RESULTS, 1-HOUR BATH.

Six Starship panels were impacted at three energy levels (500, 600, and 1100 in.-lb) and then C-scanned for damage area. The first round of thermal cycling was completed between the temperature ranges of -65° and 180°F, to mimic a typical commercial transport aircraft GAG cycle. Milestones were established for these panels to reach 500, 1000, and 2000 thermal cycles. Visual inspection and NDI were completed after each milestone was reached. The environmental chamber was constantly monitored during thermal cycling. Table 1 shows the damage area after each cycle. The damage area does not correlate very well with impact energy. That is consistent with what was observed in this type of testing.

Table 1. Starship Panels No Loading Damage Area

Panel Name	Specimen	Impact Energy (in.-lb)	Damage Area (in^2), Thermally Cycled Panels, No Mechanical Load				
			0	500	1000	2000	5000
Panel B	B5	500	20.03	30.50	23.44	25.70	27.68
	B14	500	24.34	25.96	29.74	29.72	32.86
	B16	1100	24.60	30.43	32.55	32.60	33.94
Panel C	C14	600	34.73	35.52	35.53	36.27	36.89
	C10	1100	31.75	33.93	31.98	36.44	37.19
	C15	1100	31.33	32.04	35.12	36.65	37.23

Figure 19 shows the damage area results obtained from thermally cycling the Starship panels with three different impact energies and four stages of thermal cycling milestones: 0, 500, 1000, and 2000 GAG cycles. The damage area grew with increased cycles and then the growth stabilized. There was approximately a 20% increase in the damage area, but nothing sizeable to suggest fluid ingression was propagating catastrophically. The growth in damage as a percentage of original damage appears to be the same irrespective of both how large the damage was initially and of impact energy. On examining Starship panel B16 (figure 20), there are distinct areas visible on the C-scan. The darker area in the center of the image is crushed core, and the darkest area shows where the core is separated from the facesheet. There are two images in figure 20; the black-and-white image is a true NDI scan from the NDT automation equipment. The red added to the second scan is used to highlight the damaged areas, crushed core, or defects. A defect is visible in the upper-left corner of this scan. The defect was not included in the damaged area as it was assumed it was there from the beginning. The decrease in the damage area is a result of measurement accuracy and scatter.

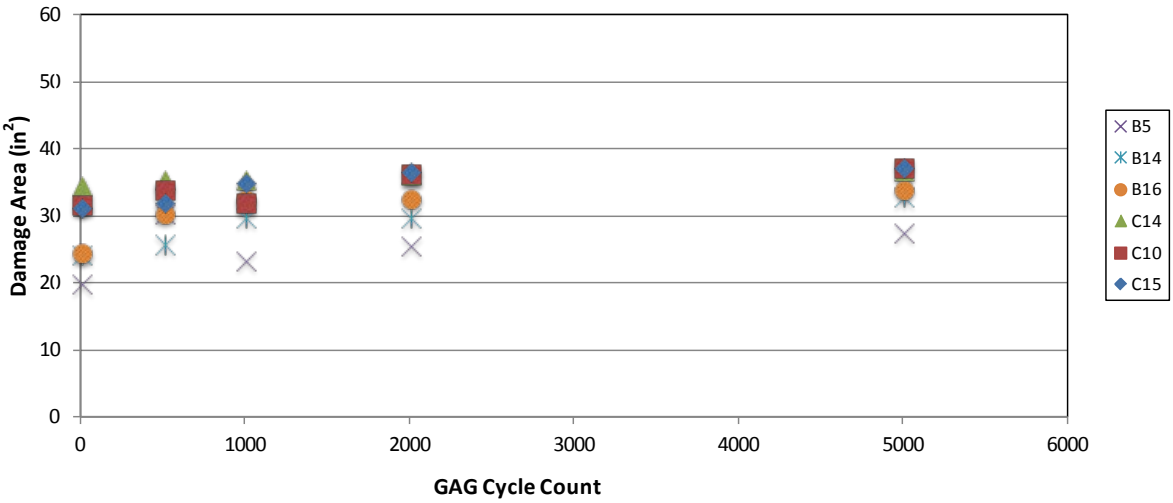

Figure 19. Damage Area vs. GAG Cycle Count for Starship Panels

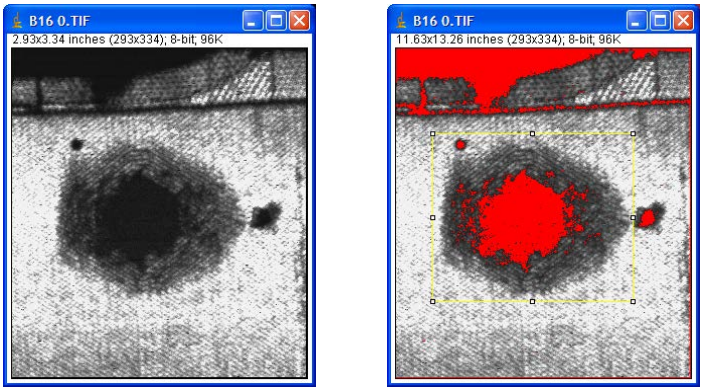

Figure 20. Starship Panel B16 Damaged Area, 0 Thermal Cycles

After 2000 thermal cycles were completed on the same Starship panel, the damaged area that increased was the additional breakage caused by the freeze/thaw cycles, as shown in figure 21 by

the red color. This is better shown by a postmortem section taken through the center of the panel (figure 22). The initial impact damage caused core microcracking outside the crushed core area, which was not detected by the NDI. After the freeze/thaw cycles, these microcracks expanded and became visible by the NDI (figure 21).

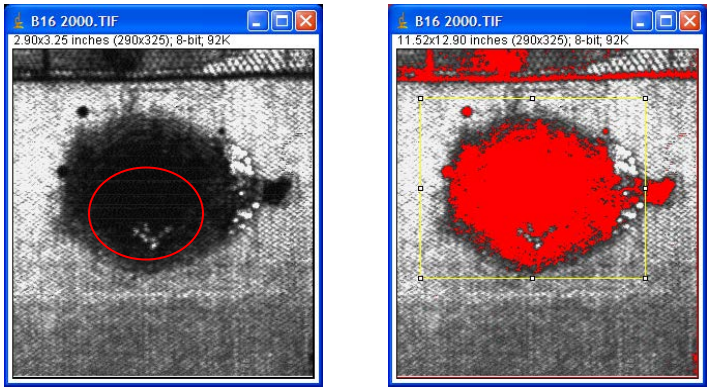

Figure 21. Starship Panel B16 Damaged Area, 2000 Thermal Cycles

The NDI images in figure 21 show the increase in the damaged area. The red, circled area has a spotty white area that actually appears slightly reflective when scanning on the NDT automation equipment. This is water that is still present in the sample after being removed from thermal cycling. This trapped water is an indication that there would have been more core damage if the panel continued cycling.

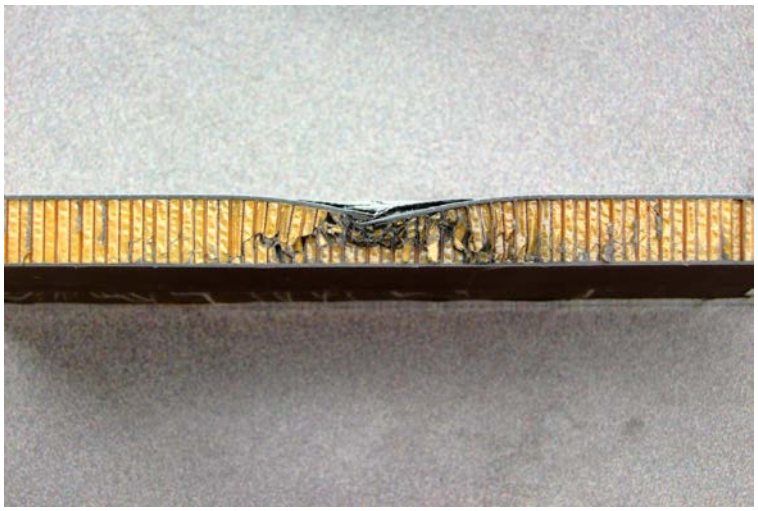

Figure 22. Cross-Section of a Typical Damaged Panel Before GAG Cycling (1100-in.-lb impact)

4.2 ADAM PANEL RESULTS, 1-HOUR BATH.

Eight Adam panels were selected and impacted at four energy levels (500, 600, 800, and 1100 in.-lb). Table 2 shows the damage area that was present after impact and thermal cycling.

Table 2. Adam Panels No Loading Damage Area

Panel Name	Specimen	Impact Energy (in.-lb)	Damage Area (in^2), Thermally Cycled Panels, No Mechanical Load				
			0	500	1000	2000	5000
CP1B	CP1B 8D	500	22.74	24.81	24.11	25.40	26.55
	CP1B 7D	600	21.16	25.46	24.58	25.07	26.29
CP2	CP2 2C	800	23.44	27.93	27.52	27.61	28.69
CP3	CP3 6B	500	20.23	21.27	20.96	22.45	22.83
CP4	CP4 2D	1100	26.80	29.29	28.57	32.00	31.80
	CP4 6C	1100	26.58	28.98	28.34	29.75	29.61
CP6	CP6 4D	1100	20.63	21.86	21.18	24.86	25.84
	CP6 8C	1100	22.19	22.58	23.18	24.08	24.47

There were no anomalies in these area measurements; no Adam panels appeared to retain more water than the Starship panels. Figure 23 shows these results.

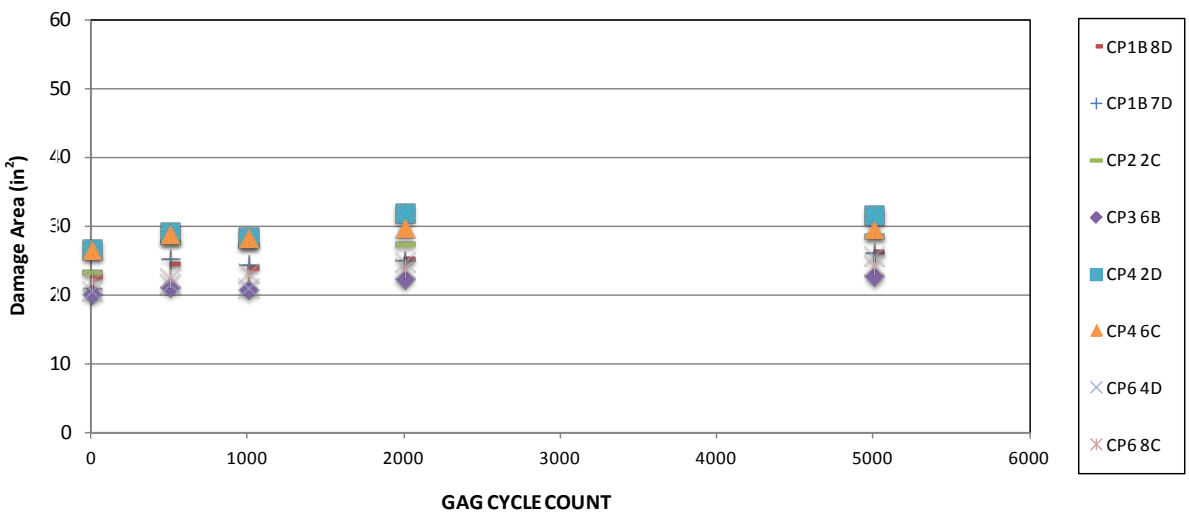

Figure 23. Damage Area vs. GAG Cycle Count for Adam Panels

Similar to the Starship panels, the Adam panels showed growth in the damage area up to 2000 cycles with arrestment after thermal cycling.

As shown in figure 24, the initial crushed core area for Adam panel CP3 6B was 20.23 in^2. This was before any thermal cycling. The crushed core was caused from the impact damage alone. The darker area shows crushed core, and the lighter gray area shows a delamination.

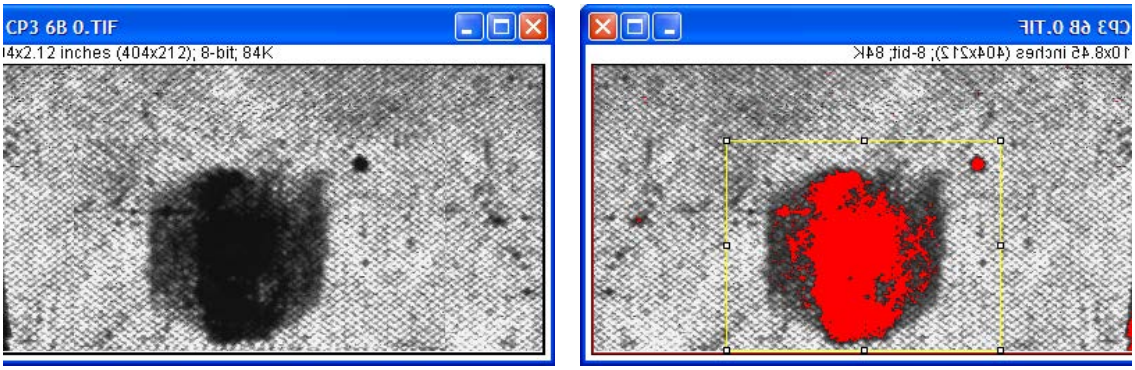

Figure 24. Adam Panel CP3 6B, 0 Thermal Cycles

Figure 25 shows that after 2000 thermal cycles on panel CP3 6B, the crushed core area grew to 23.93 in^2, which is a growth of 3.70 in^2. This is not as significant as Starship panel B16; however, it is significant enough to report that the 2000 thermal cycles completed on CP3 6B induced fluid ingression.

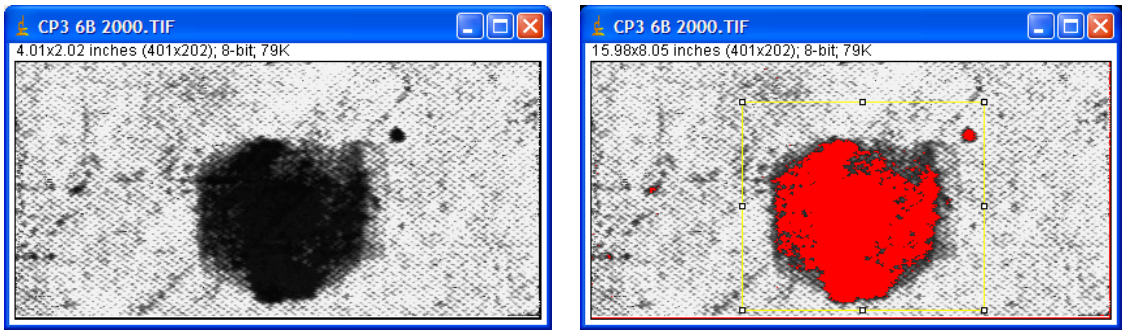

Figure 25. Adam Panel CP3 6B, 2000 Thermal Cycles

Adam Panel CP6 4D is shown in figures 26 and 27. As a result of impact damage, the initial damage area for this panel was 10.86 in^2. After 2000 thermal cycles, the damage area of crushed core increased to 14.11 in^2, a total increase of 3.25 in^2. Both Adam panels experienced less core damage from thermal cycling than the Starship panel. Also, the Adam panels did not show trapped fluid after thermal cycling. However, all three Adams panels experienced damaged core growth and minor facesheet delamination around the original damaged area as a result of thermal cycling.

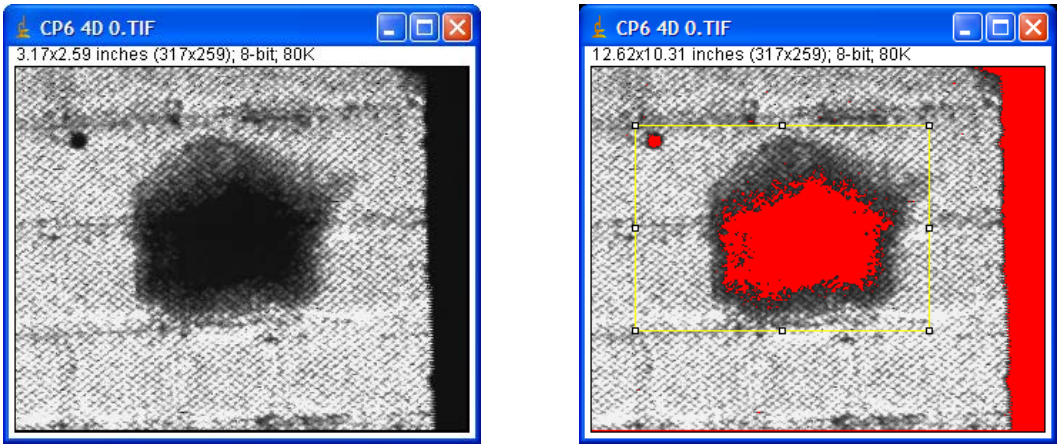

Figure 26. Adam Panel CP6 4D, 0 Thermal Cycles

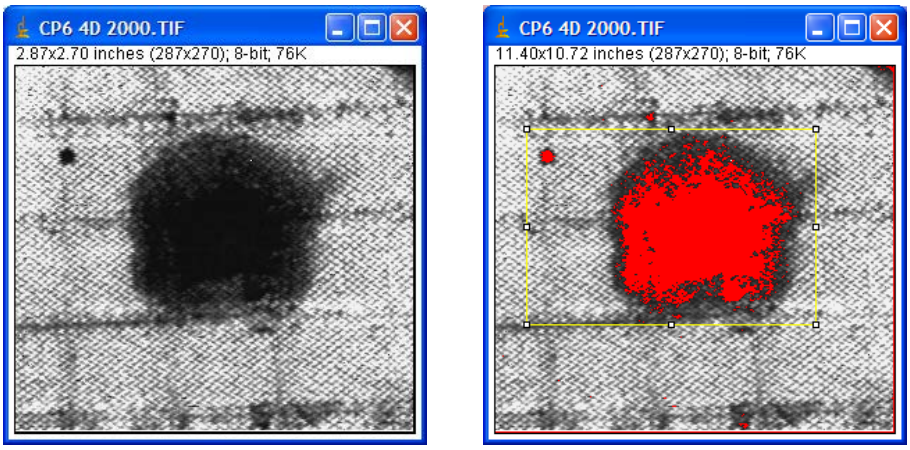

Figure 27. Adam Panel CP6 4D, 2000 Thermal Cycles

4.3 STARSHIP AND ADAM PANELS UNDER THERMAL CYCLING, 2-HOUR BATH.

The 2-hour bath results for the Starship and Adam panels are shown in tables 3 and 4 and figures 28 and 29. The results are very similar to those shown previously for the 1-hour bath.

Table 3. Starship Panels Test Results Under Thermal Cycling and 2-Hour Bath

Panel Name	Specimen	Impact Energy (in.-lb)	Dry Weight (g)	Weight After 2-Hour Water Bath at 180°F (g)	Weight After 2000 Thermal Cycles	Damage Area (in^2), Thermally Cycled Panels, No Mechanical Load				
						0	500	1000	2000	5000
Panel E	E13	600	821.40	834.60	822.00	34.27	33.95	34.10	38.36	39.95
	E18	800	925.30	937.60	924.30	32.73	39.52	37.24	39.20	41.96
Panel F	F14	600	1054.40	1081.50	1047.00	31.62	34.21	35.82	36.15	38.37
	F7	800	914.10	929.60	911.00	21.42	23.81	24.84	24.41	26.09
	F23	1100	1173.70	1179.20	1164.40	37.46	41.36	44.96	46.15	46.28

Table 4. Adam Panels Test Results Under Thermal Cycling and 2-Hour Bath

Panel Name	Specimen	Impact Energy (in.-lb)	Dry Weight (g)	Weight After 2-Hour Water Bath at 180°F (g)	Weight After 2000 Thermal Cycles	Damage Area (in^2), Thermally Cycled Panels, No Mechanical Load				
						0	500	1000	2000	5000
CP4	CP4 8C	500	450.17	479.49	471.28	22.92	24.15	24.02	28.27	28.10
	CP4 6C	1100	531.61	577.19	552.36	26.58	28.98	28.34	29.75	34.16
CP7	CP7 C3	500	492.92	545.17	514.14	29.66	29.46	35.52	32.76	33.20
	CP7 D3	800	442.82	482.8	435.48	22.81	26.71	26.91	27.70	27.25

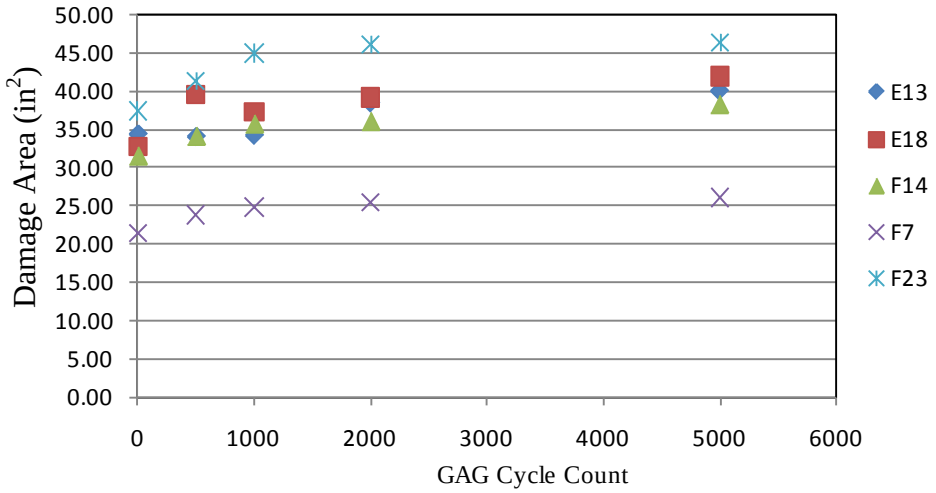

Figure 28. Damage Area vs. Cycles for Starship Panels, 2-Hour Bath

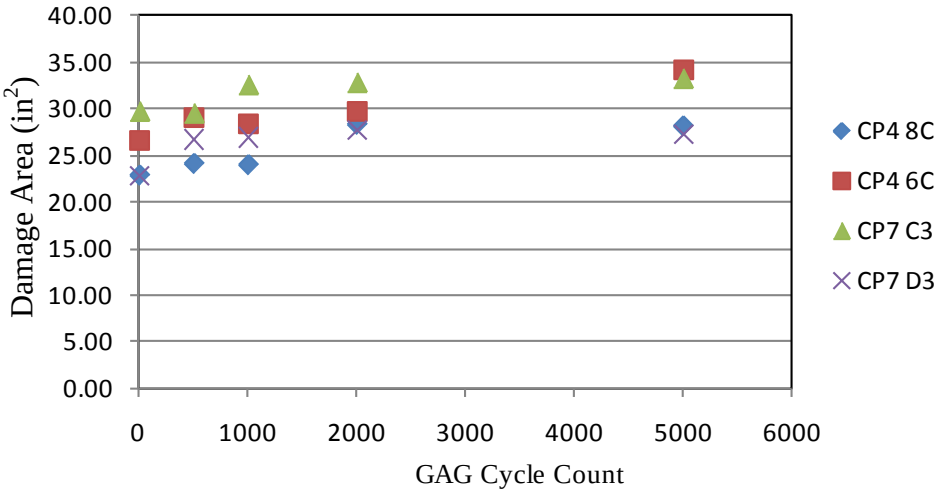

Figure 29. Damage Area vs. Cycles for Adam Panels, 2-Hour Soak

4.4 STARSHIP AND ADAM PANELS UNDER LOAD AND THERMAL CYCLING.

The next set of panels were thermally cycled after impact damage and tested under mechanical load. These stresses were induced using a four-point bend fixture that applied tension during thermal cycling in the environmental chamber. Figure 30 shows a simple free-body diagram of the loading and a top view of the fixture and how the torque is applied to induce mechanical stresses.

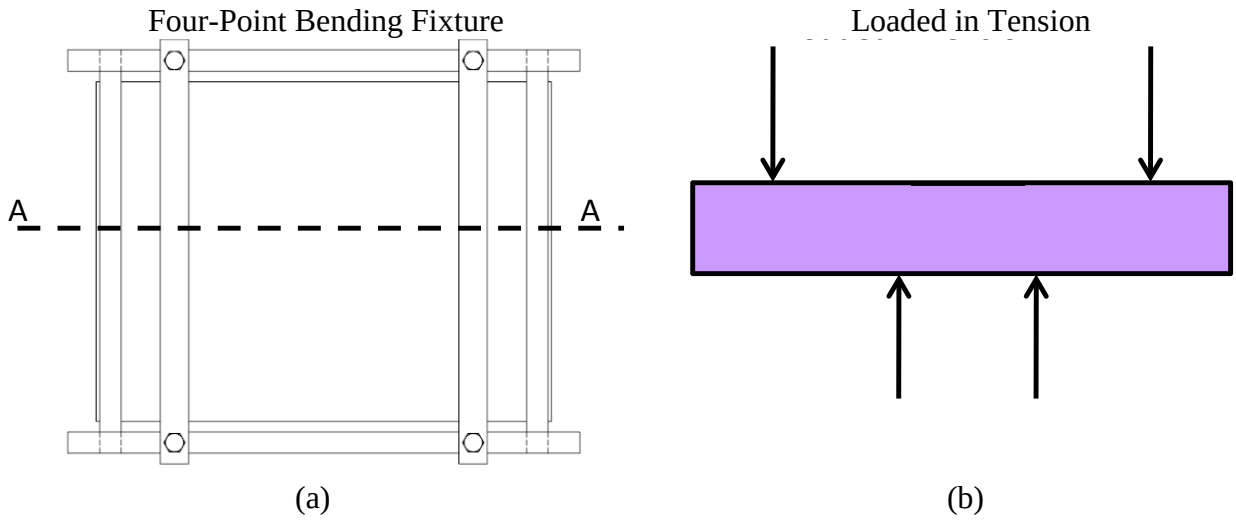

Figure 30. The (a) Four-Point Bend Fixture and (b) Free Body Diagram

All panels placed in this fixture were preloaded to 800 microstrains, but the load was not significant enough to create more damage to the panel prior to thermal cycling. One strain gage was used to ensure that the load was maintained.

Test results are summarized in table 5 for the Starship panel. This is the only panel that did not use rubber dams to contain the water around the damage; instead, the water was added between cycles as needed. This panel was sustained to 5000 cycles. Figure 31 shows that there was damage growth after the initial 1000 cycles and that the growth stabilized.

Table 5. Starship Panel C11 Results Under Load

Panel Name	Specimen	Impact Energy (in.-lb)	Loaded in Tension, Four-Point Bend Fixture, 800 Microstrains, Thermal Cycled (-65° to 180°F)				
			0	500	1000	2000	5000
Panel C	C11	1100	31.21	37.13	38.33	X	38.87

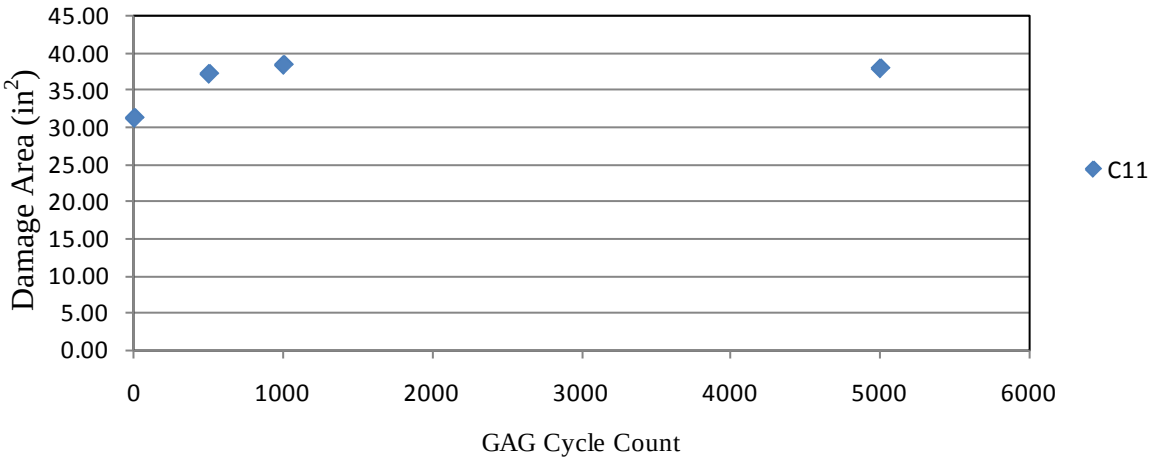

Figure 31. Damage Area vs. Cycles for the Starship Panel C11, Under Load

Starship panel C11 (figure 32), impacted at 1100 in.-lb, shows a damage area of 31.21 in^2 prior to thermal cycling. The white spots on the NDI scan are fluid accumulation in the honeycomb cells from the water used during ultrasonic inspection. Figure 33 shows Starship panel C11 impacted at 1100 in.-lb after 500 GAG cycles had been completed. The damage increased to 37.13 in^2. Again, the white spots on the scan are water accumulation in the honeycomb cells, from either the ultrasonic inspection process or the thermal cycling. The damaged area circled on the black-and-white image is the location of strain gage that was not removed entirely. This area was excluded from the damage area calculation. After 500 GAG cycles, the damage area increased by 5.92 in^2.

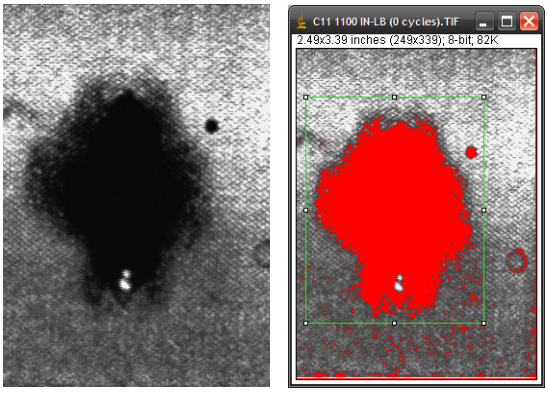

Figure 32. Starship Panel C11 After Impact, 0 Thermal Cycles

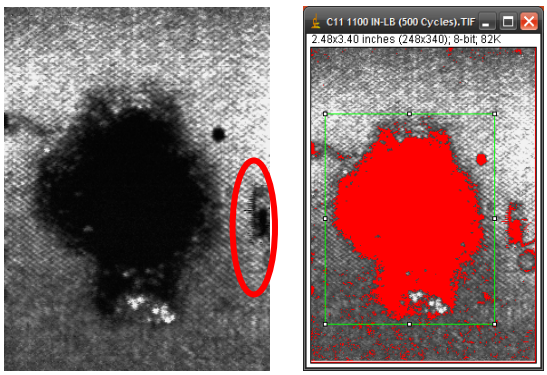

Figure 33. Starship Panel C11 After Impact, 500 Thermal Cycles

Figure 34 shows Starship panel C11, which was impacted at 1100 in.-lb, after 1000 GAG cycles had been completed, causing a new damage area of 38.33 in^2. The white spots and strain gage are still excluded from the damage area calculation. After 1000 GAG cycles the damage area increased by 7.12 in^2 from the initial damage measurement without any thermal cycling. Figure 35 shows Starship panel C11 impacted at 1100 in.-lb after 5000 GAG cycles had been completed, causing a new damage area of 37.87 in^2. The white spots and strain gage are still excluded from the damage area calculation. After 5000 GAG cycles, the damage area increased by 6.66 in^2 from the initial damage measurement without any thermal cycling.

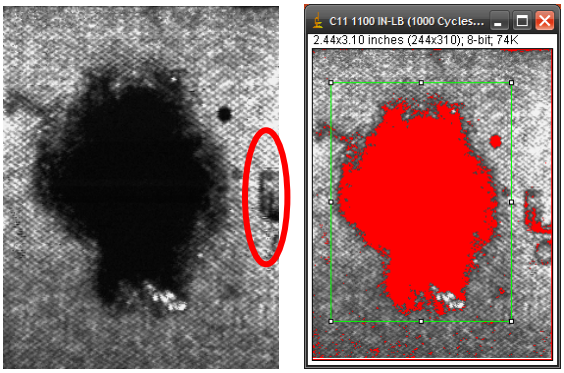

Figure 34. Starship Panel C11 After Impact, 1000 Thermal Cycles

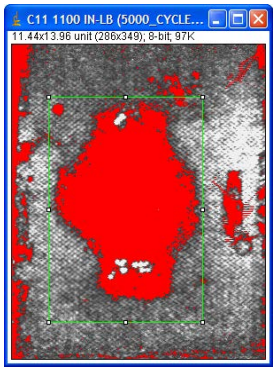

Figure 35. Starship Panel C11 After Impact, 5000 Thermal Cycles

The test data for the Starship and Adam panels that were cycled in the thermal shock chamber with rubber dams are shown in table 6.

Table 6. Starship and Adam Panels; Four-Point Loading, Thermal Cycle Results

Starship Fuselage					
Panel Name	Specimen	Impact Energy (in.-lb)	Loaded in Tension, Four-Point Bend Fixture, 800 Microstrains, Thermal Cycled (-65° to 180°F)		
Rubber Dam Used to Keep Water Localized Around Damage Area			0	100	500
Panel B	B12	500	33.93	35.11	35.20
Panel C	C14	500	12.64	12.07	12.40
	C18	800	25.22	26.11	26.13
Adam Fuselage Representative Panels					
CP3	CP3 2D	500	15.92	16.19	16.20
CP8	CP8 C6	800	28.01	32.53	32.51
	CP8 B4	1100	24.97	29.15	29.05

These panels were subjected to only 500 cycles. The reduction in cycles was justified, as most of the panels tested previously had an increase in damage at low-cycle levels. Test results are shown in table 6 and in figures 36 and 37 for the Starship and Adam panels, respectively.

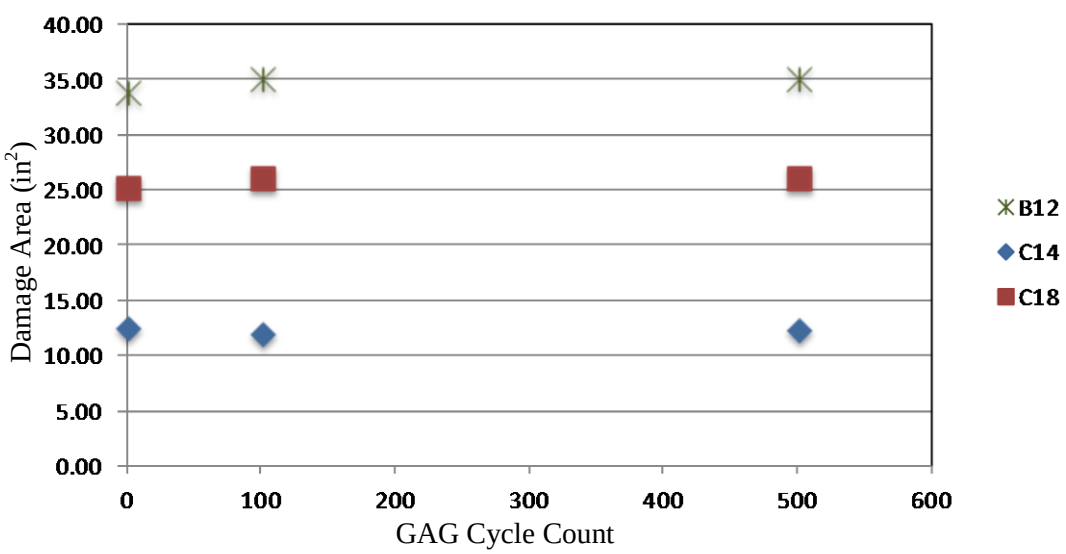

Figure 36. Damage Area vs. Cycles for Starship Panels Under Load

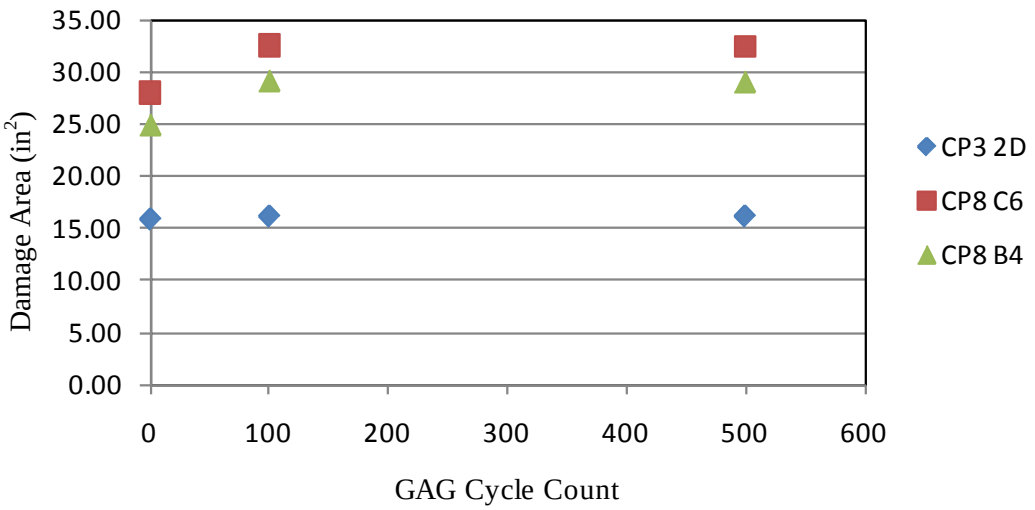

Figure 37. Damage Area vs. Cycles for Adam Panels Under Load

Starship panel C14 (figure 38) also used a rubber dam bonded to the top facesheet of the sandwich panel to contain the fluid to the damaged area. The panel was impacted at 500 in.-lb. At 0 GAG cycles, the measured damaged area was 12.64 in^2, at 100 GAG cycles, the measured damaged area was 12.07 in^2; and after 500 GAG cycles, the measured damaged area increased to 12.40 in^2. Since the area of a panel cannot decrease over time, the total damage area growth is negligible.

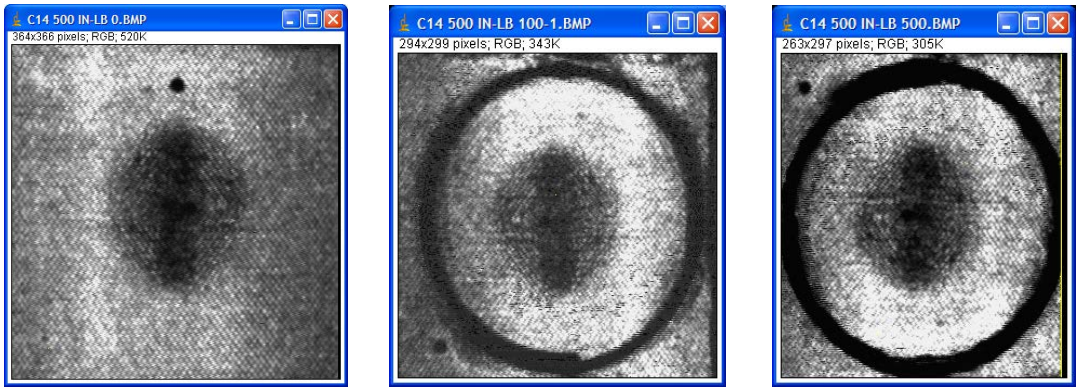

Figure 38. Starship Panel C14; 0, 100, and 500 GAG Cycles

Starship panel C18 (figure 39) also used a rubber dam bonded to the top facesheet of the sandwich panel to contain the fluid to the damaged area. The panel was impacted at 800 in.-lb. At 0 GAG cycles, the measured damaged area was 25.22 in^2; at 100 GAG cycles, the measured damaged area was 26.11 in^2; and, after 500 GAG cycles, the measured damaged area increased to 26.13 in^2. This panel had a total damage area growth of 0.91 in^2.

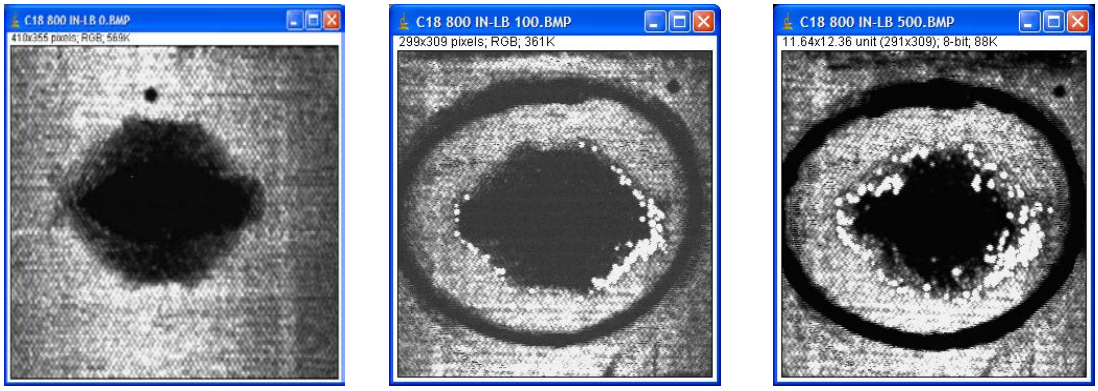

Figure 39. Starship Panel C18; 0, 100, and 500 GAG Cycles

Starship panel B12 (figure 40) also used a rubber dam bonded to the top facesheet of the sandwich panel to contain the fluid to the damaged area. The panel was impacted at 1100 in.-lb. At 0 GAG cycles, the measured damaged area was 33.93 in^2; at 100 GAG cycles, the measured damaged area was 35.11 in^2; and after 500 GAG cycles, the measured damaged area increased to 35.20 in^2. This panel had a total damage area growth of 1.27 in^2.

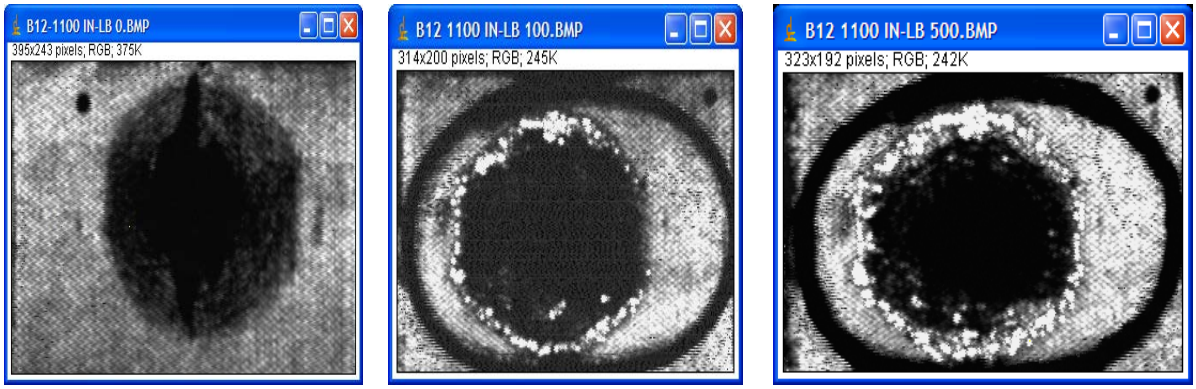

Figure 40. Starship Panel B12; 0, 100, and 500 GAG Cycles

Adam panel CP3 2D (figure 41) used a rubber dam bonded to the top facesheet of the sandwich panel to contain the fluid to the damaged area. The panel was impacted at 500 in.-lb. At 0 GAG cycles, the measured damaged area was 15.92 in^2; at 100 GAG cycles, the measured damaged area was 16.19 in^2; and after 500 GAG cycles, the measured damaged area increased to 16.20 in^2. This panel had a total damage area growth of 0.28 in^2.

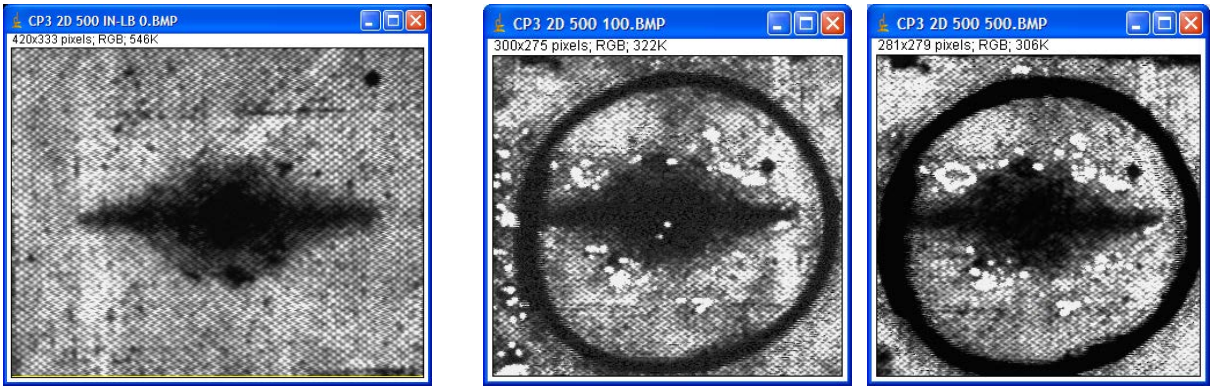

Figure 41. Adam Panel CP3 2D; 0, 100, and 500 GAG Cycles

Adam panel CP8 C6 (figure 42) also used a rubber dam bonded to the top facesheet of the sandwich panel to contain the fluid to the damaged area; the panel was impacted at 800 in.-lb. At 0 GAG cycles, the measured damaged area was 28.01 in^2; at 100 GAG cycles, the measured damaged area was 32.53 in^2; and after 500 GAG cycles, the measured damaged area increased to 32.51 in^2. This panel had a total damage area growth of 4.52 in^2; this growth occurred prior to the 500 GAG cycles being completed.

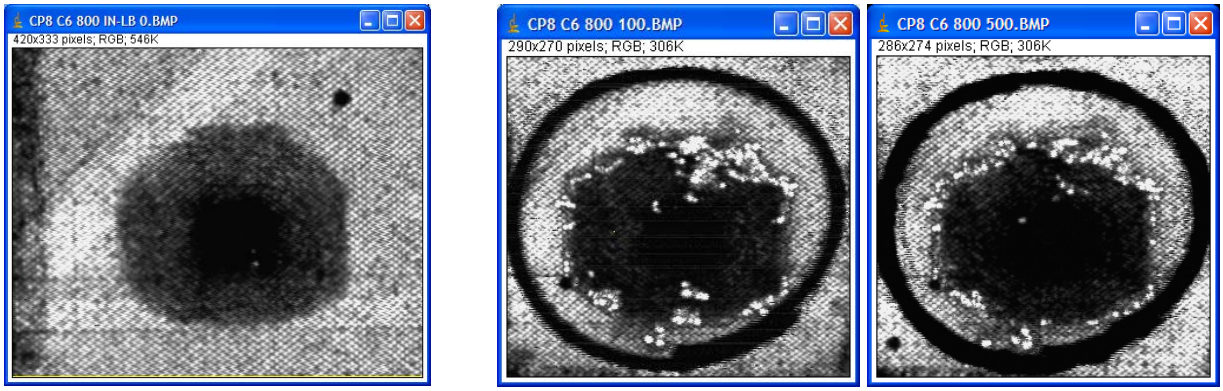

Figure 42. Adam Panel CP8 C6; 0, 100, and 500 GAG Cycles

Adam panel CP8 B4 (figure 43) also used a rubber dam bonded to the top facesheet of the sandwich panel to contain the fluid to the damaged area. The panel was impacted at 1100 in.-lb. At 0 GAG cycles, the measured damaged area was 24.97 in^2; at 100 GAG cycles, the measured damaged area was 29.15 in^2; and after 500 GAG cycles, the measured damaged area increased to 29.05 in^2. This panel had a total damage area growth of 4.18 in^2; this growth occurred prior to the 500 GAG cycles being completed.

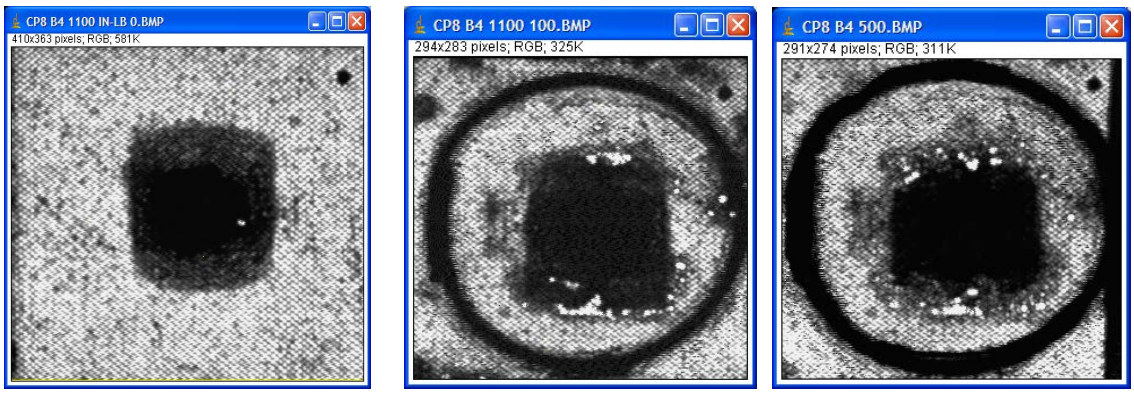

Figure 43. Adam Panel CP8 B4; 0, 100, and 500 GAG Cycles

5. CONCLUSIONS.

This research focused on how impact damage propagates with ingested moisture under thermal ground-air-ground cycles. This research was completed using representative skins from two aircraft: a Starship sandwich skin and a manufactured A700 Adam Aircraft panel that matches a more current airframe design.

The Starship and Adam panels were cycled using an environmental chamber with a traditional cycle that ramped between nominal temperatures of -65° and 180°F. Test results showed approximately 20% damage growth after 1000 cycles, after which the damage did not increase. The additional damage was core breakage resulting from the initial core cracks expanding under freeze/thaw cycles. This was true for no-load panels, 1- and 2-hour baths, and for panels under load. The Starship panels actually showed slightly more damage area growth than the Adam panels. This may be an effect of the manufacturing times of the two sets of panels: the Adam panels are manufactured with more current manufacturing techniques than the Starship panels.

It should be noted that immersing the test panels in a hot water bath is quite aggressive compared to a typical airplane service environment. This is a realistic environment the damage might grow less and stabilize sooner. Ultrasonic inspection was the inspection technique for measuring and analyzing the damage growth after thermal cycling the panels. The test panels in this research had trapped water in the damage area that slightly affected the actual damage area calculation. Since the panels sat in a water bath before each cycle and were exposed to water during cycling and again when undergoing ultrasonic inspection, there are several possibilities for how water was trapped in the sandwich panel. With ultrasonic inspection, there is also some error in the range of the scanning equipment, and sandwich panels often encounter this as a result of their honeycomb cell structure more than solid laminates. The gross nondestructive inspection does not differentiate between core wall damage, core crushing, or facesheet to core delamination and, thus, some sectioning was performed to clarify the damage growth and mode.

6. FUTURE WORK.

The effect of pressure on fluid ingression is another area that needs to be studied. Additionally, a fixture needs to be designed to simulate internal cabin pressure against the fuselage skins and

then atmospheric pressure pushing back on the outside of the fuselage while undergoing thermal cycling.

A continuous fluid supply during thermal and mechanical loading, water baths, and presoaking the panels may not be enough to mitigate the fluid ingression growth and propagation. Providing a constant fluid supply to the damaged test panel while exposed to thermal and mechanical loads will uncover exactly what is occurring during service.

Laboratory tests using a three-dimensional scanning electron microscope, which defines crack details using a liquid-dye penetrant to trace the crack details in a composite sandwich structure, may be an adequate inspection method. This may also aid in the understanding of the fluid path and propagation.

7. REFERENCES.

1. Shafizadeh, J.E., Seferis, J.C., Chesmar, E.F., and Geyer, R., "Evaluation of the In-Service Performance Behavior of Honeycomb Composite Sandwich Structures," ASM International, Vol. 8, No. 6, 1999, pp. 661-668.

2. "Airline Maintenance Facility Cuts Repair Costs While Improving Part Quality," *High Performance Composites*, May 2004, http://www.compositesworld.com/articles/airline-maintenance-facility-cuts-repair-costs-while-improving-part-quality.

3. Whitehead, S., McDonald, M., and Bartholomeusz, R.A., "Loading, Degradation and Repair of F-111 Bonded Honeycomb Sandwich Panels—Preliminary Study," Defense Science & Technology Organization (DSTO)—TR-1041, Melbourne, Australia: DSTO Aeronautical and Maritime Research Laboratory, August 2000, http://www.dtic.mil/cgi-bin/GetTRDoc?AD=ADA385139.

4. Cise, D.M. and Lakes, R.S., "Moisture Ingression in Honeycomb Core Sandwich Panels: Directional Aspects," *Journal of Composite Materials*, Vol. 31, No. 22, 1997, pp. 2249-2262.

5. Scholz, D.B, et al., "Advanced Technology Composite Fuselage—Materials and Processes," NASA Contractor Report 4731, April 1997.

6. Glass, D.E., et al., "Honeycomb Core Permeability Under Mechanical Loads," NASA Contractor Report 206263, December 1997.

7. Loken, H.Y., et al., "Water Ingression Resistant Thin Faced Honeycomb Cored Composite Systems With Facesheets Reinforced With Kevlar Aramid Fiber and Kevlar With Carbon Fibers," E.I. DuPont de Nemoursa & Company, Inc., Wilmington, Delaware, 1988.